**Pharmacogn.** Mag.
A multifaceted peer reviewed journal in the field of Pharmacognosy and Natural Products
www.phcog.com | www.phcog.net

ORIGINAL ARTICLE

# Binding of Metronidazole to *Enterococcus faecalis* Homoserine Kinase: Binding Studies, Docking Studies, and Molecular Dynamics Simulation Studies

**Harpreet Singh, Satyajeet Das, Pramodkumar P Gupta[1], Sagar Batra, Richa Prakash, Vijay Kumar Srivastava, Anupam Jyoti, Vikas Gupta[2], S. L. Kothari, Sanket Kaushik**

Amity Institute of Biotechnology, Amity University, Jaipur, Rajasthan, [1]School of Biotechnology and Bioinformatics, DY Patil Deemed to be University, Navi Mumbai, Maharashtra, [2]Department of Biotechnology, DAV College, Amritsar, Punjab, India

Submitted: 13-Mar-2020 Revised: 05-May-2020 Accepted: 06-Jul-2020 Published: 30-Nov-2020

## ABSTRACT

**Background:** *Enterococcus faecalis* (*Ef*) is an opportunistic virulent bacterial pathogen resistant to a diverse class of antibiotics by possession of a wide range of resistance mechanisms. **Aim and Objective:** Looking at the increasing number of infections caused by *Ef*, it is essential to develop alternative strategies to fight against *Ef*. In this regard, homoserine kinase (HSK) is an important enzyme of threonine biosynthesis pathway in *Ef*. Threonine is an essential amino acid, and HSK catalyzes the formation of O-phospho-L-homoserine production, which is an important step in threonine metabolism. Therefore, *Enterococcus faecalis* homoserine kinase (*Ef*HSK) becomes an ideal target for antimicrobial drug development. **Methodology:** We report binding studies, docking studies, and molecular dynamics (MD) simulation studies of *Ef*HSK. Fluorescence spectroscopy studies indicated the binding of metronidazole with *Ef*HSK. **Result:** Docking studies further showed that amino acid residues such as Asn124 and Gly83 in the phosphate-binding loop of *Ef*HSK play a vital role in the formation of H-bonds with the ligand metronidazole. The site where ligand was bound is a deep groove, which is regarded as the binding cavity of the protein. Docking studies were further confirmed by MD simulation studies. **Conclusion:** Metronidazole might be considered as a potential inhibitor of *Ef*HSK, as this occupies the binding pocket and eventually can reduce the kinase activity of this enzyme.

**Key words:** *Enterococcus faecalis* homoserine kinase purification, *in silico* modeling, molecular docking, molecular dynamic simulation, spectrofluorimetric binding assay

## SUMMARY

- The study was planned to identify the binding of metronidazole with *Ef*HSK and to further analyze the nature of interaction and the binding site of the metronidazole on *Ef*HSK. It was performed to identify metronidazole as a potential inhibitor, which can block the activity of *Ef*HSK. *Ef*HSK is an important protein involved in threonine biosynthesis pathway. We have used fluorescence spectroscopy techniques to find binding of metronidazole to *Ef*HSK. A computer-aided approach was used to identify the interaction between *Ef*HSK and metronidazole. It is proposed that this molecule can have a significant inhibitory property against *Ef*HSK by binding to the catalytic site of the protein.

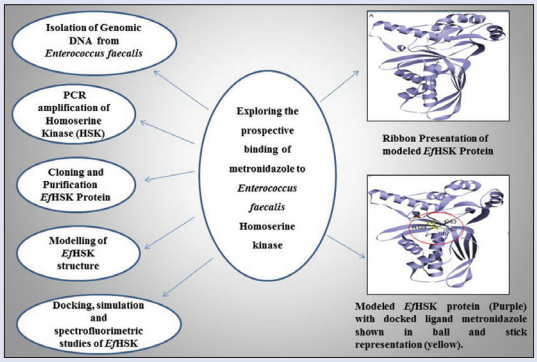


**Abbreviations used:** *Ef*: *Enterococcus faecalis*; HSK: Homoserine kinase; *Ef*HSK: *Enterococcus faecalis* homoserine kinase; MD: Molecular dynamics; HSK-ADP: Homoserine kinase-Adenosine diphosphate; PCR: Polymerase chain reaction; RMSD: root mean square deviation

**Correspondence:**

Dr. Sanket Kaushik,
Amity Institute of Biotechnology, Amity University Rajasthan, Jaipur, India.
E-mail: sanketkaushik@gmail.com

**DOI:** 10.4103/pm.pm_99_20

**Access this article online**
**Website:** www.phcog.com
**Quick Response Code:**

## INTRODUCTION

Over the past few decades, *Enterococcus faecalis* (*Ef*) has been recognized as an important opportunistic bacterial pathogen possessing a wide range of resistance mechanisms.[1,2] *Ef* is an anaerobic Gram-positive, catalase-negative, low Guanine and Cytosine (GC) containing coccoid bacterium generally found in a hospital environment.[3] Extensive use of commercially available antibiotics in hospitals has contributed to the dissemination and emergence of nosocomial enterococcal infections,[4] including urinary tract infections,[5] endocarditis,[6] and soft-tissue infections,[7] especially in emergency wards and intensive care units.[8] Along with increasing antibiotic resistance, the rise in nosocomial infections is also due to the ability of *Ef* to form biofilms on diagnostic instruments and visceral organs.[9] *Ef* is resistant to several classes of antimicrobial agents, which includes aminoglycosides,[10] β-lactams,[2] and quinolones;[11] hence, *Ef* infections are difficult to treat. Therefore, it has become imperative to identify new drug targets and develop new antimicrobial agents against *Ef*. Homoserine kinase (HSK; EC.2.7.1.39) is one of the key enzymes in threonine biosynthesis pathway



**Cite this article as:** Singh H, Das S, Gupta PP, Batra S, Prakash R, Srivastava VK, *et al*. Binding of metronidazole to *Enterococcus faecalis* homoserine kinase: Binding studies, docking studies, and molecular dynamics simulation studies. Phcog Mag 2020;16:S553-60.

as it performs the first step after the branch point to methionine. It belongs to GHMP kinase superfamily and catalyzes adenosine triphosphate (ATP)-dependent phosphorylation of L-homoserine to O-phospho-L-homoserine, which is essential for the synthesis of protein in bacterial species.[12,13] Consequently, HSK from *Enterococcus faecalis* homoserine kinase (*Ef*HSK) forms a potential drug target. So far, the structure of *Ef*HSK is not available, although the crystal structure of HSK from several bacterial species has been solved, which includes *Methanocaldococcus jannaschii*,[12] *Corynebacterium glutamicum*,[14] *Agrobacterium fabrum* (PDB: 2PPQ), *Cytophaga hutchinsonii* (PDB: 4P52), and *Mycobacterium abscessus* (PDB: 6CYZ). It has been reported that under optimum physiological conditions, HSK exists as a homodimer with two active sites.[15,16] The crystal structure of HSK and HSK-adenosine diphosphate (HSK-ADP) complex reported a unique nucleotide-binding fold, which may be involved in the binding of ATP, that are highly conserved in several GHMP kinases. It has been suggested that the highly conserved sequence motif among GHMP kinases is motif 2 with consensus $PX_3GSSAA$.[12] In this regard, looking at the vital role of *Ef*HSK in the metabolic pathway of bacteria, it becomes important to study the structural details of *Ef*HSK for designing novel antibacterial compounds. Here, we report the cloning, expression, and purification of HSK from *Ef.* Binding studies of metronidazole and *Ef*HSK were performed using fluorescence spectroscopic studies. *In silico* modeling of *Ef*HSK protein was performed to generate the three-dimensional (3D) model; molecular docking studies of *Ef*HSK were also done to identify the interaction between the metronidazole and *Ef*HSK. In addition to this, to evaluate the docking stability and flexibility of the complex, a molecular dynamics-based study was carried out. Compound metronidazole showed significant interactions with the protein.

## MATERIALS AND METHODS

### Bacterial strains and growth conditions

*Escherichia coli* DH5α strain was used as a cloning host and BL21 (DE3) for expression of the recombinant proteins. Cultures were grown in Luria–Bertani (LB) broth or solid medium with 50 μg/ml kanamycin at 310 K.

### Plasmid construction

The *Ef*thrB gene encodes a 287-residue polypeptide, with a molecular weight of 31.5 kDa. It was amplified from *Ef* genomic DNA as a template by the polymerase chain reaction (PCR) using forward (HSKf: 5'-ggaattcCATATGatgaaaataagagtacctgcc-3') and reverse primers (HSKr: 5'-ccgCTCGAGttaaaagacttgaacaccttct-3'). The forward primer contained the restriction site of NdeI and the reverse primer contained the restriction site of XhoI. PCR product was cloned in pET28a vector, and T4 DNA ligase (Thermo, CA, USA) was used in the ligation reaction, which was set up at 277 K overnight.

### Expression and purification of homoserine kinase proteins

The resulting plasmid (pET28a + *Ef*HSK = pHSK) was transformed into the *E. coli* strain BL21 (DE3) competent cells for expression studies. The bacterial strain was cultured in LB broth (HiMedia, Mumbai, India) containing kanamycin (HiMedia, Mumbai, India) 50μg/ml at 310 K with shaking at 130 rev/min. Expression of HSK was induced to an absorbance of 0.6 at 600 nm with 0.4 mM isopropyl β-D-1-thiogalactopyranoside at 293 K overnight in shaker incubator (130 rev/min). The uninduced and induced cells were harvested by centrifugation at 8000g for 15 min. A cell pellet was suspended in 18 ml B-PER-II bacterial protein extraction reagent (Thermo, CA, USA) to lyse the cells. The lysed cells were centrifuged for 11000g for 15 min at 277 K, and the pellet was discarded. All purification steps were conducted at 277 K. The overexpressed protein was purified with Ni-NTA resin (Qiagen, Hilden, Germany) column pre-equilibrated with buffer A consisting of 150 mM sodium chloride, 50 mM Tris. Initially, 50 ml buffer A was used for washing, accompanied by washing with 50 ml buffer B consisting of 150 mM sodium chloride, 50 mM Tris, and 30 mM imidazole. The protein was eluted with 15 ml buffer C consisting of 150 mM sodium chloride, 50 mM Tris, and 300 mM imidazole, which was concentrated using a protein concentrator of 10 K MWCO (Thermo, CA, USA). The final purification step was desalting using a dextran desalting column (Thermo, CA, USA). After that, the protein was further concentrated using concentrator, and for further analysis, the protein was stored at 253 K.

### *In silico* modeling of *Enterococcus faecalis* homoserine kinase protein

In order to get the homologous structure of HSK, a specified PDB BLAST is performed in the Swiss-MODEL server. Numerous homologous structures were reported on the basis of sequence similarity, out of which the structure is made based on query coverage and identity which altogether results in a total score (including E-value). Therefore, the homolog is made in correlation with *Listeria monocytogenes* (PDB ID: 3HUL) as a template using Swiss-MODEL workspace (https://swissmodel.expasy.org).[17]

### Structure assessment and validation

The theoretical model of protein structure needs to be assessed and validated for their poor quality of folding patterns and higher energy conformation. Here, we have considered the Ramachandran plot and Protein Structure Analysis (ProSA) analysis to assess and validate our modeled protein structure. The template, which was used for structure validation, was reported as a monomeric structure determined by X-ray diffraction method at 2.19 Å resolution as deposited in RCSB (https://www.rcsb.org/). The template-target alignment mode program builds with ProMod3 version 1.3.0 of Swiss-MODEL server, which was carried out with a $Q_{mean}$ value of the structure accordingly. Ramachandran plot was calculated using PROCHECK in PDBSUM platform[18] and ProSA analysis was carried out for both template and modeled structure to calculate the structural error and energy. ProSA tool was used for structure-based assessment of generated structure.[19,20] Finally, the structure was visualized using Discovery Studio Visualizer software (Dassault Systemes BIOVIA, Discovery Studio Visualizer, Release 2017, San Diego: Dassault Systemes, 2016), and Pymol was used to align the template and modeled structure to calculate the structural differences.

### Docking studies of modeled *Enterococcus faecalis* homoserine kinase with ligand

Before docking, the modeled protein is energy based optimized by solvating the protein in a water box and implemented default conjugate gradient energy minimization method under NAMD;[21] for 10000 iterations, results are analyzed using VMD.[22]

AutoDock tools[23] were used in the docking of HSK with its ligand. The 3D structure of ligand of L-homoserine and metronidazole was obtained from the PubChem database (https://pubchem.ncbi.nlm.nih.gov). Using AutoDock, the torsional root of the ligand was detected to make it suitable for the rotation and also equalizing the charge and atoms. At the same time, the protein is also prepared by adding Kollman charges and required H-atoms, and after preparing both the protein and

ligand, the grid box was generated of dimensions 100 × 106 × 126 Å in the respective XYZ direction with the spacing of 0.375 Å. To validate the binding affinities of the ligand with the modeled protein structure, the Broyden–Fletcher–Goldfarb–Shanno-based AutoDock Vina tool was used to generate eight possibilities of the ligand and then judged on the basis of root-mean-square deviation (RMSD) and binding affinity (Kcal/mol).

## Molecular dynamics

In order to gain the insight of *Ef*HSK and metronidazole complex interactions, we have submitted the complex of metronidazole for molecular dynamics simulation-based studies using Gromacs version 2019.1.[24] The protein topology files are created using Charmm27 force field using TIP3P water model. In order to generate topology for ligand, initially, it was first converted to Sybyl.mol2 format using Avogadro tool by adding hydrogens,[25] and parameters were calculated using the online generation tool CGENFF.[26] The parameters for topology and coordinates of protein and ligand were merged, and an independent system is generated. The system was solvated using 14,205 solvent components as water and counter ions were added to neutralize the number of $Na^+$ ions in the dodecahedron box. The solvated system was energy minimized by employing the steepest descent algorithm for 10,000 steps and was employed to remove any bad contacts and steric clashes of protein–ligand complexes. The system was equilibrated at a constant temperature of 300 K and NVT (amount of substance, N, volume, V and temperature,T) was performed by 100 ps and NPT (amount of substance, N, pressure, P and temperature ,T) ensemble was carried out for 100 ps. The final molecular dynamics (MD) production run was carried out at 1 bar pressure and 300 k for 15,000,000 runs equivalent to 30 ns. Visualization is carried out using VMD and DS visualizer 2019.

## Binding studies using fluorescence spectroscopy

Fluorescence measurements were carried out for analyzing the binding studies of *Ef*HSK protein with metronidazole using fluorescence spectroscopy (LS55, PerkinElmer, Waltham, MA, USA). Scanning experiments were conducted by maintaining the entrance and exit slit widths at 9nm at a speed of 200 nm/min. *Ef*HSK was excited at wavelength 280 nm, and emission spectra were measured within the range of 300–550 nm at 298 K. The concentration of *Ef*HSK was kept constant at $1 \times 10^{-8}$ M, and the concentration of metronidazole was varied as 10 µl, 20 µl, 30 µl and 40 µl, which was prepared from $1 \times 10^{-7}$ M stock solution. The spectral changes of *Ef*HSK, thus obtained with various concentrations of ligands, were recorded and plotted. The least-square fit intensity changes for *Ef*HSK-metronidazole binding curve were obtained using SigmaPlot 14.0. Each experiment was performed thrice, and its average value was used for data analyses.

# RESULTS

## Cloning, overexpression, and purification of *Enterococcus faecalis* homoserine kinase protein

Amplified *Ef*thrB gene encoding *Ef*HSK protein was cloned, expressed, and purified using affinity chromatography. Finally, the purity of the protein was determined using sodium dodecyl sulfate–polyacrylamide gel electrophoresis (SDS-PAGE, which showed a single band around 31.5 KDa with respect to protein marker [Figure 1].

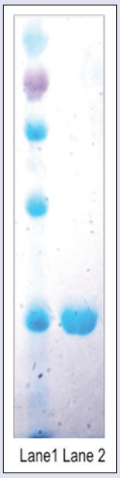


**Figure 1:** Sodium dodecyl sulfate–polyacrylamide gel electrophoresis showing the *Enterococcus faecalis* homoserine kinase Purification. Lane 1 is the protein marker. Lane 2 is purified *Enterococcus faecalis* homoserine kinase protein at around 36 kDa region with respect to the marker

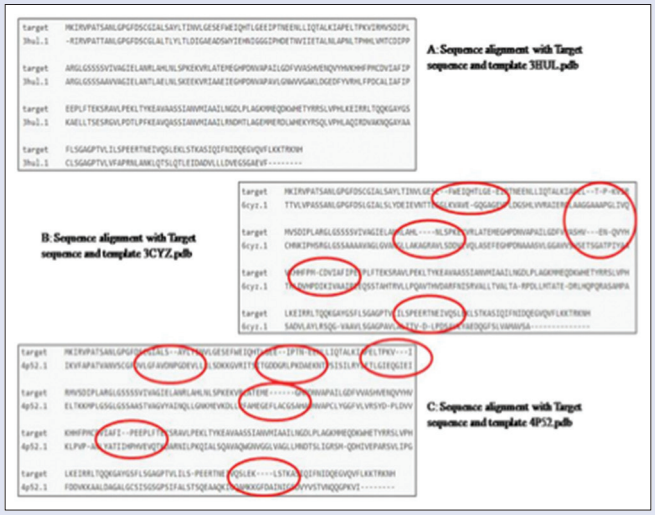


**Figure 2:** Multiple sequence alignment of the target protein and template

## *In silico* modeling and validation

The Swiss-MODEL server reported numerous homologous template structures for the given input HSK protein sequence. Out of these, numerous sequences were reported with insertion or deletion of amino

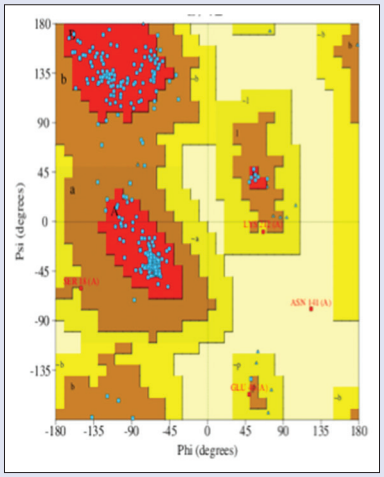


**Figure 3:** Ramachandran plot of the model *Enterococcus faecalis* homoserine kinase protein

acid residues within the target sequence [Figure 2]. Comparing the target sequence with template (PDB ID: 3HUL) alignment, no insertion or deletion is identified in between the sequence except at –N and –C terminal ends, whereas in comparison to templates, 3CYZ and 4P52 numerous insertion/deletion are reported. Hence, the protein structure of HSK modeled from the coordinates of *L. monocytogenes* (PDB ID: 3HUL) has a maximum identity of 56.45%, with query coverage of 100%, with a maximum score of 348 with the least E-value of $6e^{-121}$. Ramachandran plot analysis exhibited a 285 total amino acid as 99.6% of residues falling under the favored and allowed region and 1 amino acid residue, i.e., 0.4% as outliers, significantly validates the integrity of the model [Figure 3]. Figure 4a and b exhibits ribbon representation and surface diagram of *Ef*HSK. The report generated through Swiss-MODEL server represents the availability of the structural motif $PX_3GSSAA$ and the phosphate-binding loop, which thereby enhanced the authenticity of the model. However, the sequence alignment was carried out by ClustalW, which favors the sequential motif at the same. The Z-score for the template structure 3HUL-Chain A is -7.72 and lies within the core high-resolution structural data [Figure 5a] with low energy-based conformation [Figure 5b]. The modeled structure reported a Z-score of −8.7 and reported the X-ray high confidence zone [Figure 5c] with better low energy-based conformation in comparison to template structure [Figure 5d]. The RMSD between template structure and modeled structure alignment scored 0.11 A [Figure 5e].

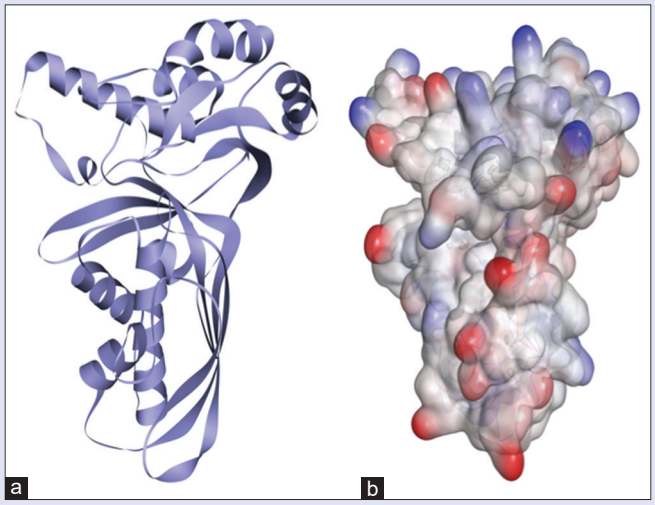


**Figure 4:** (a) Ribbon presentation of modeled *Enterococcus faecalis* homoserine kinase protein in purple color. (b) Surface diagram of modeled *Enterococcus faecalis* homoserine kinase

## Docking using the ligand

The optimized protein was evaluated on the basis of bond, angle, dihedral, improper, and total energy of the protein. The final energy of the protein exhibited to be of −48832.1346 kcal/mol after energy minimization [Figure 6 ] and show a linear trend in the energy which depicts no higher conformation in its iteration, including no changes in the bond, angle and dihedral properties.

AutoDock and AutoDock Vina tools were used in the docking of *Ef*HSK indigenous substrate L-homoserine and with the selected ligand metronidazole. After analyzing the dock models with both the ligands, we found that amino acid residues such as Asn and Gly in the phosphate-binding loop play a critical role in the formation of H-bonds, and therefore, this deep groove was regarded as the binding cavity of the protein.

The indigenous substrate of *Ef*HSK, L-homoserine, interacted within the catalytic region by forming hydrogen bonds with Ala81, Arg82, Gly83, Leu84, Gly85, Ser86, Ser87, His121 and Asn124 [Figure 7].

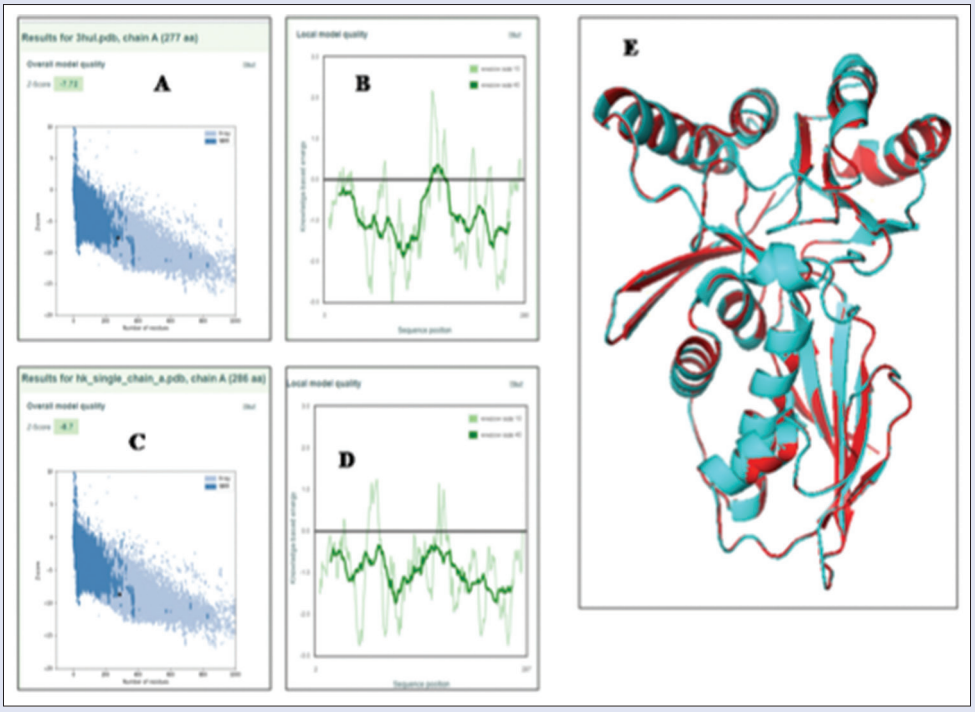


**Figure 5:** Protein Structure Analysis result and structural alignment. (A & B) ProSA value and energy for template structure 3HUL. (C & D) ProSA value and energy for modeled protein structure. (E) RMSD value of 3HUL chain A (red) and modeled structure (cyan) was determined to be 0.11 A

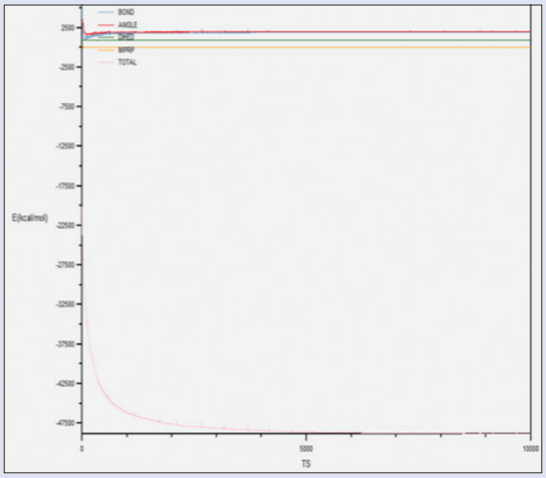

**Figure 6:** Protein-energy minimized form

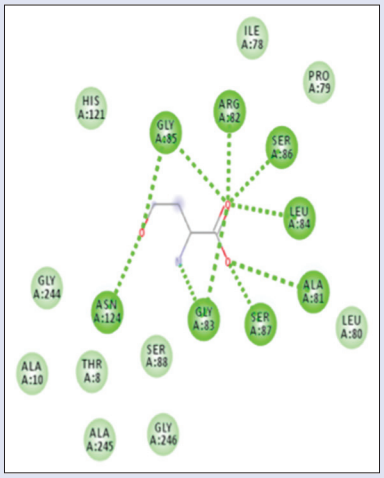


**Figure 7:** Docked structure of L-homoserine with the protein

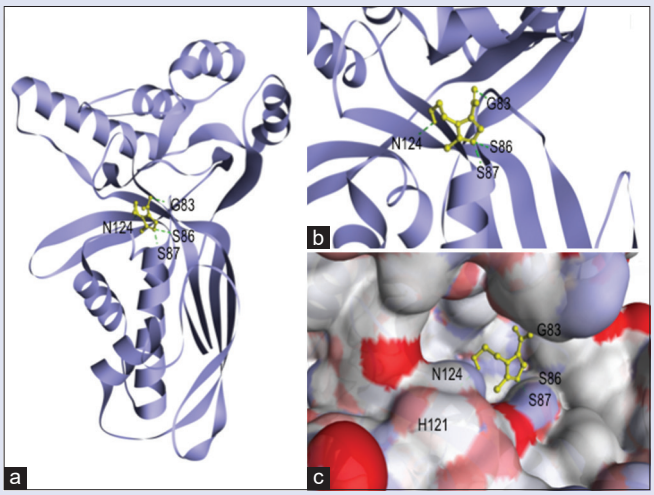


**Figure 8:** Metronidazole binding in *Enterococcus faecalis* homoserine kinase: (a) Ribbon presentation of modeled *Enterococcus faecalis* homoserine kinase protein (purple) with docked ligand metronidazole shown in ball and stick representation (yellow). (b) A close-up view of the ligand-binding site of *Enterococcus faecalis* homoserine kinase with the docked lead molecule. (c) Molecular surface diagram with ligand binding site

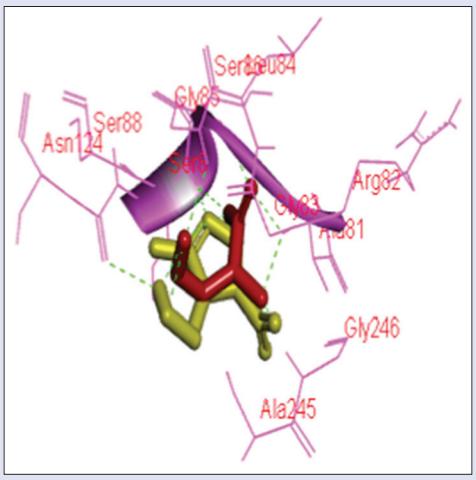


**Figure 9:** Superimposition of L-homoserine (red color) and metronidazole (yellow color) in the catalytic site of *Enterococcus faecalis* homoserine kinase protein

As for metronidazole where the docking score was calculated as −4.6 Kcal/mol very close to L-homoserine dock score, amino acids such as Gly83, Ser86, Ser87, and Asn124 participated in H-Bond formation. The ligand was found to show their close vicinity toward His121. Many other residues under the phosphate loop such as Ser86-Ser88 and Arg82 might be involved in bond formation. The docking of the ligand with modeled *Ef*HSK is shown in Figure 8 (metronidazole binding in *Ef*HSK). The close conformation study reveals the L-homoserine and metronidazole occupies a similar region of interaction within the catalytic site of *Ef*HSK protein, as stated in Figure 9 with similar pharmacophoric interactions and identical H-bond with Gly83, Ser86, Ser87, and Asn124.

## Molecular dynamics

To evaluate the docking stability and flexibility of the complex, a molecular dynamics-based study was carried out. The generated complex with all the parameters and topologies was energy wise optimized and reported potential energy was −6.841e +05 kJ/mol [Figure 10a]. We conducted time-dependent MD simulation at 30 ns using Gromacs version 2019.1. The residual deviations and fluctuation in the complexes between the protein and ligand backbone system were determined using RMSD and graphs generated using Xmgrace platform (https://plasma-gate.weizmann.ac.il/Grace/). The increasing trend was observed in (*Ef*HSK-metronidazole) complex which exhibited RMSD values 0–0.25 nm at equilibrium state (0 to 25 ns) and 0.5 nm (25 to 30 ns) at later stage [Figure 10b]. The protein reported a maximum deviation of 0.4 nm over a period of 30 ns [Figure 11a] and ligand reported a maximum deviation of 0.15 nm over a period of 30 ns [Figure 11b]. The final output has exhibited a hydrogen bond with Gly83, Leu84, Asn124, and Ala245, followed by nonbonded interactions with Leu84, Asn124, and Ala245 [Figure 10c] with a total energy of −4.82277e +05 kJ/mol. However, the common interaction retained before after the MD simulation is Gly83, and Asn124 reveals the most positive feature of binding analysis.

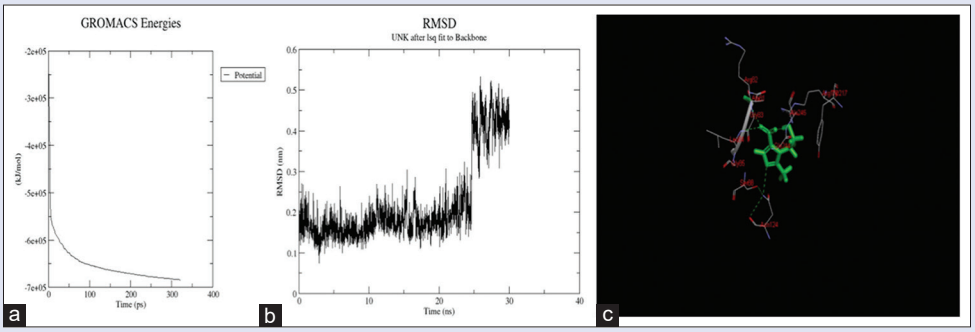


**Figure 10:** (a) Potential energy of the complex. (b) Root-mean-square deviation *Enterococcus faecalis* homoserine kinase protein–ligand metronidazole. (c) Magnified view of interaction site, hydrogen bond with Gly 83, Leu 84, Asn 124, and Ala 245 followed by nonbonded interactions with Leu 84, Asn 124, and Ala 245

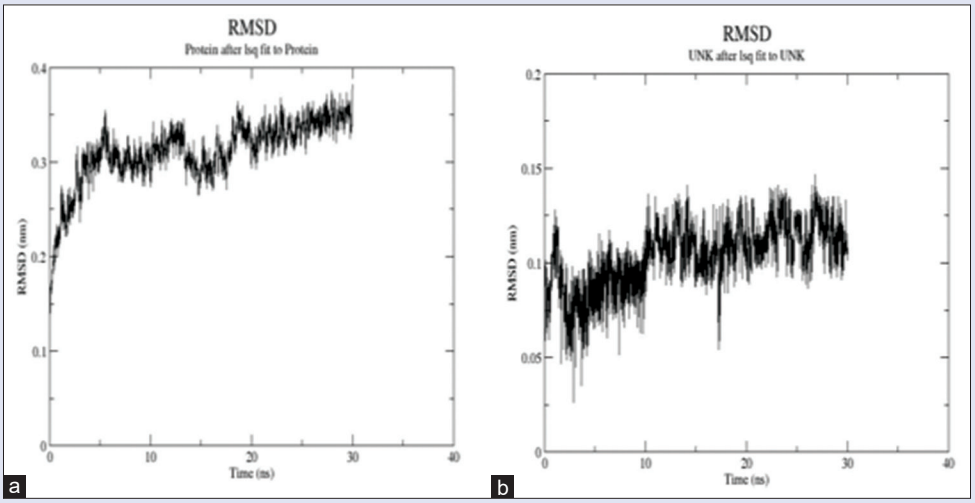


**Figure 11:** (a) *Enterococcus faecalis* homoserine kinase root-mean-square deviation. (b) Metronidazole root-mean-square deviation

## Binding studies using fluorescence spectroscopy

Binding of the ligand metronidazole with protein *Ef*HSK was determined by the decrease in fluorescent intensity with increasing concentration of ligand, while the concentration of protein was kept constant. The spectra for the *Ef*HSK with increasing ligand concentration were recorded. It was noted that the metronidazole quenched the fluorescence intensity of protein at wavelength 341 nm, which revealed that the compound bound to *Ef*HSK. The observed fluorescence measurements were further used for estimating the fluorescence quenching coefficient (Q) using:

$$Q = (F_o/F-1)$$

Where Fo and F represent the fluorescence intensities of *Ef*HSK in the absence and presence of quencher molecule, respectively. The Q% values thus obtained were plotted against the concentrations of ligands. The $R^2$ value, which provides an index of goodness of fit of the curve, was obtained using SigmaPlot 14.0 and was determined as 0.986 for metronidazole [Figure 12]. The value of equilibrium constant ($K_d$) for the binding of metronidazole was found to be $8.09 \times 10^{-9}$.

# DISCUSSION

*Ef*HSK is involved in threonine biosynthesis pathway and is ubiquitously expressed in all prokaryotic cells. It catalyzes ATP-dependent phosphorylation of L-homoserine to O-phospho-L-homoserine; it performs the first step after the branch point to methionine, which is an essential amino acid. In this study, the comparative protein modeling approach was used to solve the 3D structure of HSK, and *in silico* docking studies were done to analyze the favorable interaction between protein and ligand (metronidazole).[27-29] Docking studies showed a significant binding of ligand molecule with *Ef*HSK. It was observed that the L-homoserine and metronidazole shared a common H-bond interaction with Asn124, Gly83, Ser86, and Ser87 amino acid residues. However, many other residues under the phosphate loop such as Ser 86-Ser 88 and Arg82 might be involved in bond formation with metronidazole with a close margin difference of docking score 0.3 Kcal/mol. After analyzing the docked models, we found that amino acid residues such as Asn or Gly in the phosphate-binding loop play a critical role in the formation of H-bonds, and therefore, this deep groove was regarded as the binding cavity of the protein [Figure S1]. Thus, it can be proposed that the ligand (metronidazole) binds at the site where natural substrate L-homoserine binds [Figure 9]. As a result, this ligand may be regarded as a potential inhibitor of *Ef*HSK, as they occupy the same binding pocket and block the site, which can further reduce the activity of this enzyme. Apart from examining the stereochemical studies of the predicted model, a molecular dynamics-based study was carried out to evaluate the docking stability and flexibility of the complex. The protein–ligand interaction exhibited a hydrogen bond with Gly83, Leu84, Asn124, and Ala245, followed by nonbonded interactions with Leu84, Asn124, and Ala245 [Figure 10c] with a total energy of −4.82277e + 05 kJ/mol. However, the common

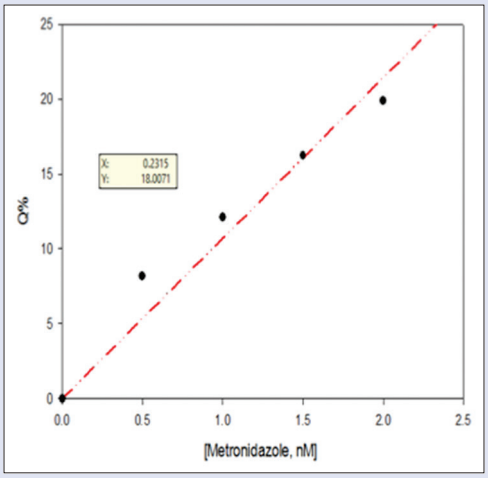


**Figure 12:** The binding curves showing bindings of metronidazole to *Enterococcus faecalis* homoserine kinase, exhibits an increase in fluorescence quenching as a concentration of the ligands increases from 10 nM to 40 nM

interaction retained before after the MD simulation is Gly83, and Asn124 reveals the most positive feature of binding analysis. In addition to this, fluorescence spectroscopy technique is widely used to study the protein–ligand interactions.[30-34] The value of $K_d$ (equilibrium constant) for binding of metronidazole was found to be $8.09 \times 10^{-9}$ M. This value showed that the ligand bound to *Ef*HSK tightly. Both docking and fluorescence studies confirmed the binding of metronidazole at the binding site of the protein. Furthermore, ligand metronidazole is a medicinal compound and has antibacterial activity. Metronidazole is an antiprotozoal and antibiotic medication.[35] It is used either alone or in combination with other antibiotics to treat anaerobic infections.[36-39] These findings encouraged us to conduct *in silico* docking to analyze the binding of these molecules with *Ef*HSK. Further, fluorescence experiment was used to validate the binding studies. *In silico* docking and fluorescence studies proved that this molecule binds to *Ef*HSK. This study provides a platform for designing more potent compounds having even better binding affinity and interactions with the protein. It can contribute toward developing new compounds with significant antibacterial activity leading to rational structure-based drug design.

## CONCLUSION

The study was planned to identify the binding of metronidazole with *Ef*HSK and to further analyze the nature of interaction and the binding site of the metronidazole on *Ef*HSK. It was performed to identify metronidazole as a potential inhibitor, which can block the activity of *Ef*HSK. *Ef*HSK is an important protein involved in threonine biosynthesis pathway. We have used fluorescence spectroscopy techniques to find binding metronidazole with *Ef*HSK. A computer-aided approach was used to identify the interaction between *Ef*HSK and metronidazole. It is proposed that this molecule can have a significant inhibitory property against *Ef*HSK by binding to the catalytic site of the protein. This compound can be used as a potential lead molecule, which can be used to treat infections caused by *Ef*.

## Financial support and sponsorship

Nil.

## Conflicts of interest

There are no conflicts of interest.

## REFERENCES

1. Hollenbeck BL, Rice LB. Intrinsic and acquired resistance mechanisms in enterococcus. Virulence 2012;3:421-33. Available from: http://www.ncbi.nlm.nih.gov/pubmed/23076243. [Last accessed on 2019 Feb 22].
2. Miller WR, Munita JM, Arias CA. Mechanisms of antibiotic resistance in enterococci. Expert Rev Anti Infect Ther 2014;12:1221-36. Available from: http://www.ncbi.nlm.nih.gov/pubmed/25199988. [Last accessed on 2019 Feb 21].
3. Fisher K, Carol P. The ecology, epidemiology and virulence of Enterococcus. Microbiology 2009;155:1749-57. Available from: http://mic.sgmjournals.org. [Last accessed on 2019 Feb 21].
4. Guzman Prieto AM, van Schaik W, Rogers MR, Coque TM, Baquero F, Corander J, *et al.* Global emergence and dissemination of enterococci as nosocomial pathogens: Attack of the clones? Front Microbiol 2016;7:788. Available from: http://www.ncbi.nlm.nih.gov/pubmed/27303380. [Last acessed on 2019 Feb 28].
5. Heintz BH, Halilovic J, Christensen CL. Vancomycin-Resistant enterococcal urinary tract infections. Pharmacotherapy 2010;30:1136-49. Available from: http://doi.wiley.com/10.1592/phco. 30.11.1136. [Last accessed on 2019 Feb 28].
6. Megran DW. Enterococcal endocarditis. Clin Infect Dis 1992;15:63-71. Available from: https://academic.oup.com/cid/article-lookup/doi/10.1093/clinids/15.1.63. [Last accessed on 2019 Feb 22].
7. Rajkumari N, Mathur P, Misra MC. Soft tissue and wound infections due to *Enterococcus* spp. among hospitalized trauma patients in a developing country. Glob Infect Dis 2014;6:189-93. Available from: http://www.ncbi.nlm.nih.gov/pubmed/25538459. [Last accessed on 2019 Feb 28].
8. Richards MJ, Edwards JR, Culver DH, Gaynes RP. Nosocomial infections in combined medical-surgical intensive care units in the United States. Infect Control Hosp Epidemiol 2000;21:510-5. Available from: https://www.cambridge.org/core/product/identifier/S0195941700043137/type/journal_article. [Last accessed on 2019 Feb 22].
9. Sava IG, Heikens E, Huebner J. Pathogenesis and immunity in enterococcal infections. Clin Microbiol Infect 2010;16:533-40. Available from: https://linkinghub.elsevier.com/retrieve/pii/S1198743X14616876. [Last accessed on 2019 Feb 22].
10. Courvalin P. Genetics of glycopeptide resistance in Gram-positive pathogens. Int J Med Microbiol 2005;294:479-86. Available from: https://www.sciencedirect.com/science/article/abs/pii/S1438422104001365. [Last accessed on 2019 Feb 22].
11. Lopez M, Tenorio C, del Campo R, Zarazaga M, Torres C. Characterization of the mechanisms of fluoroquinolone resistance in vancomycin-resistant enterococci of different origins. J Chemother 2011;23:87-91. Available from: http://www.tandfonline.com/doi/full/10.1179/joc.2011.23.2.87. [Last accessed on 2019 Mar 23].
12. Krishna SS, Zhou T, Daugherty M, Osterman A, Zhang H. Structural basis for the catalysis and substrate specificity of homoserine kinase. Biochemistry 2001;40:10810-8. Available from: http://www.ncbi.nlm.nih.gov/pubmed/11535056. [Last accessed on 2019 Feb 22].
13. Zhou T, Daugherty M, Grishin NV, Osterman AL, Zhang H. Structure and mechanism of homoserine kinase. Structure 2000;8:1247-57. Available from: http://linkinghub.elsevier.com/retrieve/pii/S0969212600005335. [Last accessed on 2019 Feb 22].
14. Petit C, Kim Y, Lee SK, Brown J, Larsen E, Ronning DR, *et al.* Reduction of Feedback Inhibition in Homoserine Kinase (ThrB) of *Corynebacterium glutamicum* Enhances l-Threonine Biosynthesis. ACS Omega 2018;3:1178-86. Available from: http://pubs.acs.org/doi/10.1021/acsomega. 7b01597. [Last acessed on 2019 Feb 22].
15. Burr B, Walker J, Truffa-Bachi P, Cohen GN. Homoserine kinase from *Escherichia coli* K12. Eur J Biochem 1976;62:519-26.
16. Theze J, Kleidman L, St. Girons I. Homoserine kinase from *Escherichia coli* K-12: Properties, inhibition by L-threonine, and regulation of biosynthesis. Bacteriol 1974;118:577-81. Available from: http://www.ncbi.nlm.nih.gov/pubmed/4364023. [Last accessed on 2019 Feb 22].
17. Biasini M, Bienert S, Waterhouse A, Arnold K, Studer G, Schmidt T, *et al.* SWISS-MODEL: Modelling protein tertiary and quaternary structure using evolutionary information. Nucleic Acids Res 2014;42:W252-8. Available from: http://academic.oup.com/nar/article/42/W1/W252/2435313/SWISSMODEL-modelling-protein-tertiary-and. [Last accessed on 2019 Feb 28].
18. Laskowski RA. PDBsum new things. Nucleic Acids Res 2008;37:D-355-9. Available from: https://www.ncbi.nlm.nih.gov/pmc/articles/PMC2686501/. [Last accessed on 2020 May 28].

19. Markus Wiederstein MJ. ProSA-web: Interactive web service for the recognition of errors in three-dimensional structures of proteins. Nucleic Acids Res 2007;35:407-10. Available from: https://www.ncbi.nlm.nih.gov/pubmed/17517781. [Last acessed on 2020 Mar 03].
20. Sippl MJ. Recognition of errors in three dimensional structures of proteins. Proteins Struct Funct Bioinforma 1993;17:355-62. Available from: http://doi.wiley.com/10.1002/prot.340170404. [Last acessed on 2020 Mar 03].
21. Acun B, Hardy DJ, Kale LV, Li K, Phillips JC, Stone JE. Scalable molecular dynamics with NAMD on the summit system. IBM J Res Dev 2018;62:1-9.
22. Humphrey W, Dalke A, Schulten K. VMD: Visual molecular dynamics. J Mol Graph 1996;14:33-8.
23. Trott O, Olson AJ. AutoDock Vina: Improving the speed and accuracy of docking with a new scoring function, efficient optimization, and multithreading. Comput Chem 2010;31:455-61. Available from: http://www.ncbi.nlm.nih.gov/pubmed/19499576. [Last accessed on 2019 Feb 28].
24. Kutzner C, Páll S, Fechner M, Esztermann A, de Groot BL, Grubmüller H. Best bang for your buck: GPU nodes for GROMACS biomolecular simulations. J Comput Chem 2015;36:1990-2008. Available from: http://doi.wiley.com/10.1002/jcc. 24030. [Last accessed on 2019 Nov 20].
25. Hanwell MD, Curtis DE, Lonie DC, Vandermeersch T, Zurek E, Hutchison GR. Avogadro: An advanced semantic chemical editor, visualization, and analysis platform. Cheminform 2012;4:17. Available from: https://jcheminf.biomedcentral.com/articles/10.1186/1758-2946-4-17. [Last accessed on 2019 Nov 20].
26. Vanommeslaeghe K, Hatcher E, Acharya C, Kundu S, Zhong S, Shim J, *et al.* CHARMM general force field: A force field for drug-like molecules compatible with the CHARMM all-atom additive biological force fields. J Comput Chem 2010;31:671-90.
27. Alam P, Chaturvedi SK, Anwar T, Siddiqi MK, Ajmal MR, Badr G, *et al.* Biophysical and molecular docking insight into the interaction of cytosine β-D arabinofuranoside with human serum albumin. Lumin 2015;164:123-30. Available from: https://www.sciencedirect.com/science/article/pii/S0022231315001477. [Last accessed on 2019 Mar 01].
28. Laskar K, Alam P, Khan R, Rauf A. Synthesis, characterization and interaction studies of 1,3,4-oxadiazole derivatives of fatty acid with human serum albumin (HSA): A combined multi-spectroscopic and molecular docking study. Eur J Med Chem 2016;122:72-8. Available from: http://europepmc.org/abstract/MED/27343854. [Last accessed on 2019 Mar 01].
29. Sliwoski G, Kothiwale S, Meiler J, Lowe EW Jr. Computational methods in drug discovery. Pharmacol Rev 2014;66:334-95. Available from: http://www.ncbi.nlm.nih.gov/pubmed/24381236. [Last accessed on 2019 Mar 01].
30. Das S, Srivastava VK, Parray ZA, Jyoti A, Islam A, Kaushik S. Identification of potential inhibitors of sortase A: Binding studies, *in silico* docking and protein-protein interaction studies of sortase A from *Enterococcus faecalis*. Int J Biol Macromol 2018;120:1906-16. Available from: https://www.sciencedirect.com/science/article/pii/S0141813018313552. [Last acessed on 2019 Mar 01].
31. Kaushik S, Singh N, Yamini S, Singh A, Sinha M, Arora A, *et al.* The mode of inhibitor binding to Peptidyl-tRNA hydrolase: Binding studies and structure determination of unbound and bound Peptidyl-tRNA Hydrolase from *Acinetobacter baumannii*. PLoS One 2013;8:e67547. Available from: https://www.ncbi.nlm.nih.gov/pmc/articles/PMC3701073/. [Last accessed on 2019 Mar 01].
32. Mocz G, Ross JA. Fluorescence techniques in analysis of protein-ligand interactions. Methods Mol Biol 2013;1008:169-210. Available from: http://link.springer.com/10.1007/978-1-62703-398-5_7. [Last accessed on 2019 Mar 01].
33. Siddiqi M, Nusrat S, Alam P, Malik S, Chaturvedi SK, Ajmal MR, *et al.* Investigating the site selective binding of busulfan to human serum albumin: Biophysical and molecular docking approaches. Int J Biol Macromol 2018;107:1414-21. Available from: https://www.sciencedirect.com/science/article/pii/S0141813017325114. [Last accessed on 2019 Mar 01].
34. Wang X, Guo XY, Xu L, Liu B, Zhou LL, Wang XF, *et al.* Studies on the competitive binding of cleviprex and flavonoids to plasma protein by multi-spectroscopic methods: A prediction of food-drug interaction. Photochem Photobiol B Biol 2017;175:192-9. Available from: https://www.sciencedirect.com/science/article/pii/S1011134417305080. [Last accessed on 2019 Mar 01].
35. Ingham HR, Selkon JB, Hale JH. The antibacterial activity of metronidazole. J Antimicrob Chemother 1975;1:355-61. Available from: https://academic.oup.com/jac/article-lookup/doi/10.1093/jac/1.4.355. [Last accessed on 2019 Feb 28].
36. Atia AJ. Synthesis and antibacterial activities of new metronidazole and imidazole derivatives. Molecules 2009;14:2431-46. Available from: http://www.mdpi.com/1420-3049/14/7/2431. [Last accessed on 2019 Feb 28].
37. Löfmark S, Edlund C, Nord CE. Metronidazole is still the drug of choice for treatment of anaerobic infections. Clin Infect Dis 2010;50 Suppl 1:S16-23.
38. Sheehy O, Santos F, Ferreira E, Berard A. The use of metronidazole during pregnancy: A review of evidence. Curr Drug Saf 2015;10:170-9. Available from: http://www.ncbi.nlm.nih.gov/pubmed/25986038. [Last accessed on 2019 Feb 28].
39. Stranz Marc BE. (PDF) Metronidazole (Flagyl IV, Searle); 1981. Available from: https://www.researchgate.net/publication/16171478_Metronidazole_Flagyl_IV_Searle. [Last accessed on 2019 Feb 28].

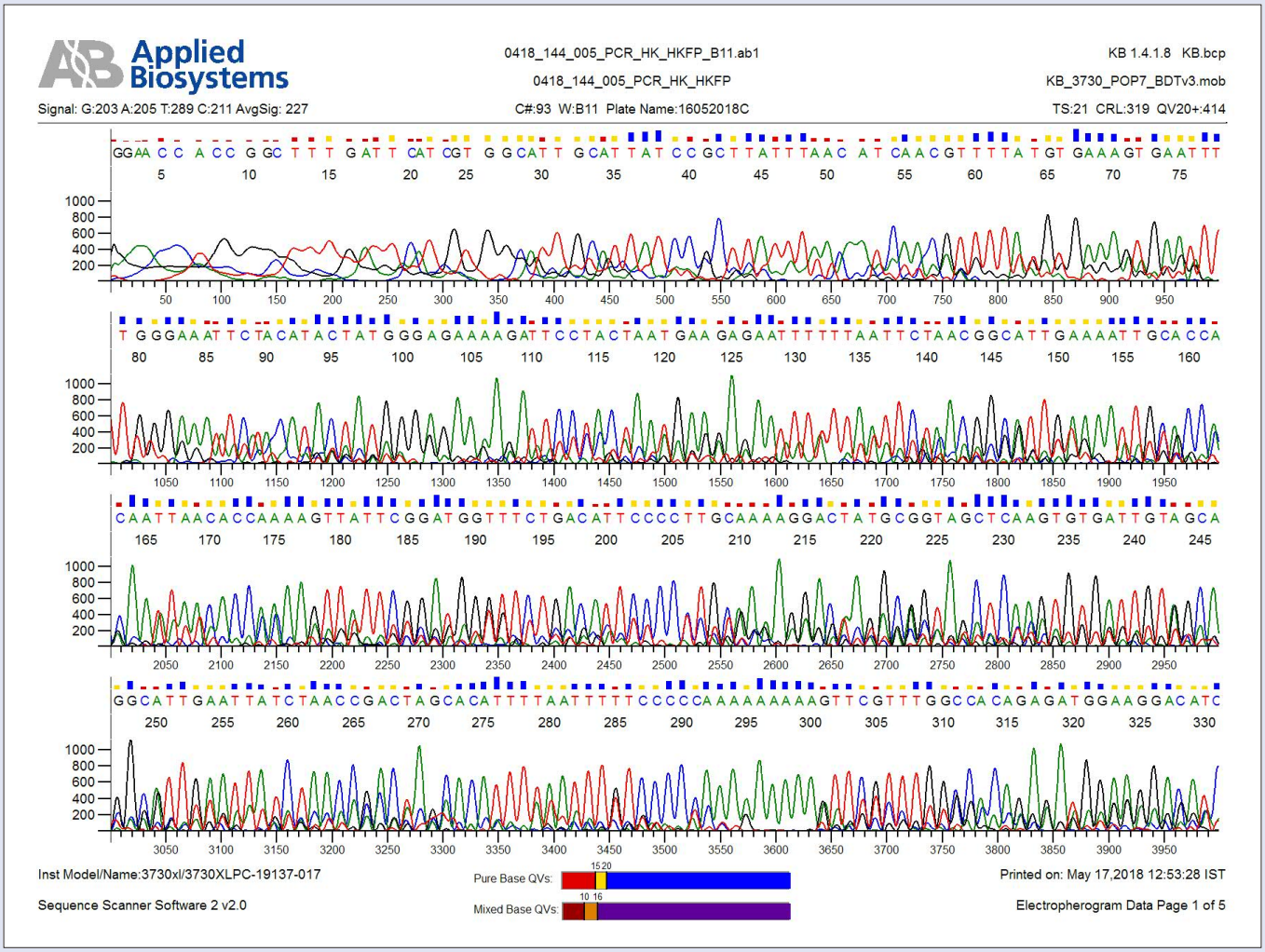


**Figure S1:** DNA sequencing data of the clone with forward and reverse frames